UNIVERSITY OF WAIKATO

Hamilton New Zealand

Spot and Futures Prices of Bitcoin: Causality, Cointegration and Price Discovery from a Time-Varying Perspective

Yang Hu, Yang (Greg) Hou and Les Oxley

Working Paper in Economics 13/19

August 2019

Corresponding Author
Les Oxley
School of Accounting, Finance & Economics
Waikato Management School
University of Waikato
Private Bag 3420
Hamilton
NEW ZEALAND
Email: les.oxley@waikato.ac.nz

Yang Hu
School of Accounting, Finance & Economics
Waikato Management School
University of Waikato
Email: yang.hu@waikato.ac.nz

Yang (Greg) Hou
School of Accounting Finance & Economics
Waikato Management School
University of Waikato
Email: greg.hou@waikato.ac.nz

Abstract

This paper investigates the causal relationships, cointegration and price discovery between spot and futures markets of Bitcoin using the daily data from a time-varying perspective for the first time in the literature. We apply the time-varying Granger causality test of Shi *et al.* (2018) to explore the causal relationship between spot and futures markets and find that futures prices Granger cause spot prices. We identify the existence of a cointegration relationship under the consideration of a time-varying cointegrating coefficient between spot and futures prices based on the Park and Hahn (1999) test. We also explore the time-varying price discovery process and find that futures prices dominate in the process, implying a leading informational role.

JEL Classification

C5, G12, G13, G14

Keywords

Bitcoin
futures
time-varying
causality
cointegration
price discovery

1. Introduction

Bitcoin was the first digital asset established in 2008 by Satoshi Nakamoto. Since then, the price of Bitcoin has increased from less than US$1 in 2010 to reach a peak of approximately US$19,000 in December 2017. During its peak in 2017, the Chicago Board Options Exchange (CBOE) and the Chicago Mercantile Exchange future markets (CME) introduced futures contracts for Bitcoin on 10 December 2017 and 18 December 2017, respectively. These two Bitcoin futures are regulated exchanges and both futures are cash-settled in US dollars.[1] On March 2019, the CBOE decided not to list additional Bitcoin futures contracts for trading and the last futures contracts expired on 19 June 2019. As a result, the CME remains the only currently traded and regulated exchange. Some comparisons of the contract specifications of the CBOE and CME markets as shown as Table 1, below.

Table 1: Some key comparisons of the CBOE and CME futures markets.

Contract Specifications	CBOE Futures	CME Futures
First Trading Date	10 December 2017	18 December 2017
Symbol	XBT	BTC
Contract Unit	1 Bitcoin	5 Bitcoin
Tick Size	$10 per contract	$25 per contract
Underlying Spot Price	The Gemini auction price from the Gemini exchange.	The Bitcoin Reference Rate from the CME.

The Bitcoin futures contracts have drawn some attention from academics. More recently, several studies have attempted to explore the price discovery in the spot and futures markets for Bitcoin. Corbet et al. (2018) apply four measures of price discovery including the information share methodology of Hasbrouck (1995), the component share of Gonzalo & Granger (1995), the information leadership measure of Yan & Zivot (2010) and the information leadership share measure of Putniņš (2013) between the CBOE and CME futures and spot prices using data sampled at a one-minute frequency. They typically find that price discovery is focused on the spot market. However, Corbet et al. (2018) use the same Bitcoin spot prices for the CBOE and CME. Kapar & Olmo (2019) conclude that the CME futures market dominates the price discovery process at the daily frequency using the price discovery measures of Gonzalo & Granger (1995) and Hasbrouck (1995) to explore the contribution of each market to the price discovery process. Kapar & Olmo (2019) use the Coindesk Bitcoin USD Price

[1] At the end of the contract, one needs to pay for the difference between the spot and futures prices of Bitcoin. There are alternative exchanges offer physically settled futures contracts using Bitcoin.

Index as the spot price. Baur & Dimpfl (2019) also investigate the price discovery of Bitcoin using the information share methodology of Hasbrouck (1995) and Gonzalo & Granger (1995) using a five-minute frequency for intradaily data. They conclude that price discovery takes place in the spot market, rather than the futures market. The transaction price of Bitstamp is used as the Bitcoin spot price in the analysis for the two futures markets. Although Corbet et al. (2018), Kapar & Olmo (2019) and Baur & Dimpfl (2019) use the same price discovery measures of Hasbrouck (1995) and Gonzalo & Granger (1995) to explore this new and interesting area using Bitcoin data, they don't produce consistent results. It should be point out that not only future contracts of the CBOE and CME are different, but their underlying spot prices are also different, see Table 1. However, this important point seems to be ignored in their empirical calculations of the information shares from the above studies.[2] The point here is that the choice of data sources for analysing pricing dynamics in Bitcoin markets is crucial, see Alexander & Dakos (2019).

Price discovery, which is generally considered to be an important indicator of the functionality futures contracts provide towards the underlying spot assets' transactions, reflects one of the major contributions of futures markets to the organization of economic activity (Silber, 1981). A number of empirical studies support the hypothesis that futures prices absorb new information first, which is then transmitted to the underlying spot market via cross-border transactions. Hence the futures market is generally regarded to lead the underlying spot price, in the long run. Supporting evidence for such assumptions have been found widely in the commodity markets and stock index markets (see, e.g., Garbade & Silber (1983), Bohl et al. (2011), Rosenberg & Traub (2009), Cabrera et al. (2009), Hauptfleisch et al. (2016), Stoll & Whaley (1990), Chan (1992), Wahab & Lashgari (1993), Ghosh (1993), Koutmos & Tucker (1996), Pizzi et al. (1998), Yang et al. (2001), Kavussanos et al. (2008); Bohl et al. (2011); among others). In this literature, the most widely-applied approaches for measuring price discovery are the Hasbrouck (1995)'s information share (IS) measure and Gonzalo & Granger (1995)'s permanent-temporary (PT/GG) measure. Both measures are based upon a framework where the unit-root (non-stationary) price series in the different markets are cointegrated. In such a framework, all the prices are driven by one common stochastic trend, which is referred to as the "permanent component" (common factor) in Gonzalo & Granger (1995) and a common efficient price in Hasbrouck (1995). In particular, the IS measure calculates the contributions of each market to the variance of the common efficient price, by accounting for both the error-correction coefficients and the information generation process. The approach is commonly applied to the examination of the price discovery of

[2] Baur & Dimpfl (2019) points out the correct spot prices for the CBOE and CME. However, due to data availability, they use the transaction price of Bitstamp as the spot price.

futures markets see for example, Booth et al. (1999), Tse (1999), Covrig et al. (2004), Ates & Wang (2005), Tse et al. (2006) and Chen & Gau (2009), among others.

The identification of the price discovery can be extended to be time variant, since the literature has found that the assimilation of information to reflect intrinsic values can evolve over time. One of the main consequences is that a time-varying variance and covariance of price innovations occurs, which refers the evolving process of information generation. Attempts to capture the time-varying information share have been recently described in the literature. There appear to be predominantly three methods established in the literature to capture the time-varying nature of price discovery. First, the time-varying information share is calculated based upon the time-varying error correction coefficients that can be derived via a rolling-window estimation on the vector error correction model (Bell et al., 2016) or a series of scaling factors imposed on the original adjustment coefficients (Taylor, 2011). The second involves calculating the information share that varies at low-frequency intervals, by using high-frequency tick data (Ates & Wang (2005); Chen & Gau (2009, 2010); Xu & Wan (2015)). Finally, Avino et al. (2015) propose to generate the time-varying information share by extending the innovation covariance matrix to be conditional on past information, where the multivariate BEKK-GARCH model is employed to estimate the conditional covariance matrix.

The informational role of a futures market has been extensively studied by investigating possible lead-lag relationships between spot and futures markets. The Granger causality is widely used to formally test for lead-lag relationships (temporal ordering) to determine which market (the spot and futures prices) leads the other. Care must be exercised here, especially the need for robustness of the results, as it is well-documented that Granger causality tests can be very sensitive to the time period of estimation or to assumptions that causal relationships do not change (time invariant) over time. As shown in Shi et al. (2019), there are many reasons to expect the existence of a time-varying casual relationship between variables of interests (e.g., changes in economic policy, regulatory structure, governing institutions, or operating environments). The procedure of Shi et al. (2018) allows practitioners to examine whether the causal relationship varies over the time, as is likely to be expected for many economic and financial variables, including Bitcoin.

In addition, the nature of the cointegrating relationship between spot and futures prices has important implications. For futures and spot markets there exists a priori expectation that there exists a strong (cointegration) relationship between the two markets. If spot and futures prices are cointegrated, spot-futures parity exists, indicating that no arbitrage opportunities arise. Moveover, the presence of cointegration also shows that futures markets are efficient. However, when testing for such conditions, conventional cointegration tests assume a static (time-invariant) framework. If this assumption is invalid, cointegration may be falsely rejected, hence, it is important to allow for a time-varying cointegration framework (where time invariance is a special case) will enriches the potential interactions between variables when they are driven by the same information set.

In this paper we seek to identify the causal, cointegration, and price discovery processes between the Bitcoin spot and futures markets, using a time-varying approach. The paper contributes to the current and fast-growing literature on Bitcoin in several key ways. First, we apply a newly developed time-varying Granger causality approach by Shi et al. (2018) to explore the causal relationship between spot and futures markets for Bitcoin. There are many advantages of the new Granger causality approach, in particular, it allows for unknown change points in the causal relationships and also takes accommodates potential heteroskedasticity which is typically ignored in the existing literature. This new testing procedure also does not require detrending or differencing of the data. Of particular interest here is that this new approach allows practitioners to identify the origination and termination dates for any episodes of causality. This new approach will be used here to study the lead-lag relationship between spot and futures markets. Second, the paper tests for potential cointegration under the time-varying cointegrating coefficient assumption using the Park & Hahn (1999) test. Previous literature on this topic takes no account of the possibility of a time-varying cointegrating coefficient. The reason why the cointegration coefficient is considered to be time-varying is consistent with the argument stated by Shi et al. (2019). In particular, Park & Hahn (1999) point out that since the cointegration reveals the long-run relationship between variables, it can not be ruled out that such relationship does not hold still throughout a long sample path given the possibility of the changing conditions of both macro and micro fundamental drivers pertaining to market operations and regulatory circumstances. Third, the paper also fills the gap of measuring price discovery in the spot and futures markets for Bitcoin by using time-varying approaches for the first time. As discussed above, current empirical studies investigate price discovery using the static (time-invariant) information share methodology. Fourth, this paper enriches the literature on empirical analysis for Bitcoin futures markets by correctly specifying the underlying spot prices for the CBOE and CME futures markets. We suggest that future research uses the correct pair of spot-futures prices for subsequent analysis. In this paper we therefore address the following three important questions from a time-varying perspective:

- Do futures prices Granger cause spot prices, or vice versa?
- Do futures prices cointegate with spot prices?
- Do futures prices lead spot prices in the price discovery process, or vice versa?

The remaining parts of the paper are organized as follows. Section 2 describes the data and econometric methods. Section 3 presents the empirical findings and Section 4 concludes.

2. Data and Method

2.1. Data

The CBOE and CME are the first two exchanges that have provided future contracts on Bitcoin. For these two futures contracts prices, we exclude the first-week data from the first trading date to avoid potential outlier data. We use the daily settlement price of the CBOE Bitcoin futures from 18 December 2017 to 16 June 2019.[3] We use the final settlement value (with a symbol of XBTS) based on Gemini auction price at 4 pm Eastern time as the spot prices for the CBOE market.[4] We also obtain the daily settlement price of the CME Bitcoin futures from 25 December 2017 to 29 July 2019. The CME Bitcoin future prices are based on the CME Bitcoin Reference Rate (BRR), which is used as a spot price for the CME market. BRR is a daily reference rate of the U.S. dollar price of one Bitcoin and developed by CME. The BRR aggregates the trade flows from the major Bitcoin spot exchanges, for example, Bitstamp, Coinbase, itBit and Kraken at 4 pm London time to ensure transparency and replicability in the underlying spot markets.[5] To construct the CBOE and CME futures price series, we only collect daily price observations of the most nearby futures contracts to ensure their liquidity. The most nearby contracts are the ones that are closest to the expiration dates at each calendar month. We switch the most nearby contract to the second most nearby one if the trading volume of the former is exceeded by the latter at the former's contract month.

The Gemini auction price and the BRR are used for representing the spot markets under consideration in this paper.[6] To align with the futures prices of Bitcoin, we then obtain the daily Gemini auction price and the BRR for the same period with the CBOE and CME futures. After matching the spot and futures data series, we end up with 416 observations for the CME sample and 393 observations for the CBOE sample. Note that our sample excludes data of weekends due to unavailability of database. Both spot and future prices are downloaded from *Thomson Reuters Datastream* for our empirical analysis. It should be pointed out that the futures and spot prices used by the CBOE and CME are different. Hence empirical analysis should be based on the counterpart spot markets.

All spot and futures prices are transformed into natural logarithms and are presented as Figure 1. As can be seen from the figure, there is a decreasing trend for both spot and futures prices from the beginning of sample period until the early February 2019, which might represent a bear market in

---

[3]More details related to the CBOE Bitcoin futures can be assessed by the website cache at https://cfe.cboe.com/cfe-products/xbt-cboe-bitcoin-futures/contract-specifications.

[4]Gemini is a digital currency exchange that founded in 2014.

[5]More details about the CME Bitcoin futures can be found from the CME website at https://www.cmegroup.com/education/bitcoin/cme-bitcoin-futures-frequently-asked-questions.html.

[6]For a discussion of the choice of spot and futures data, see Baur & Dimpfl (2019).

both the spot and futures markets. From early February 2019, both prices follow an upward trend until the end of sample period, which suggests a bull market. Second, the patterns of both spot and futures prices look similar. It is possible that there exists a long run relationship between spot and futures prices. This will be further examined via cointegration testing.

We also provide the descriptive statistics of the Bitcoin spot and futures daily returns in Table 2. As can be seen from the table, the means of spot and futures returns are negative. The volatilities of the four markets are similar. Second, returns of the four markets do not follow a normal distribution as indicated by Jarque-Bera test. This might be due to non-zero skewness and excess kurtosis, which will be further examined in a SNP approach. Finally, heteroscedasticity may exist in the spot and futures returns given the existence of significant Ljung-Box Q statistics. This issue will be addressed by using a DCC-GARCH modeling approach.

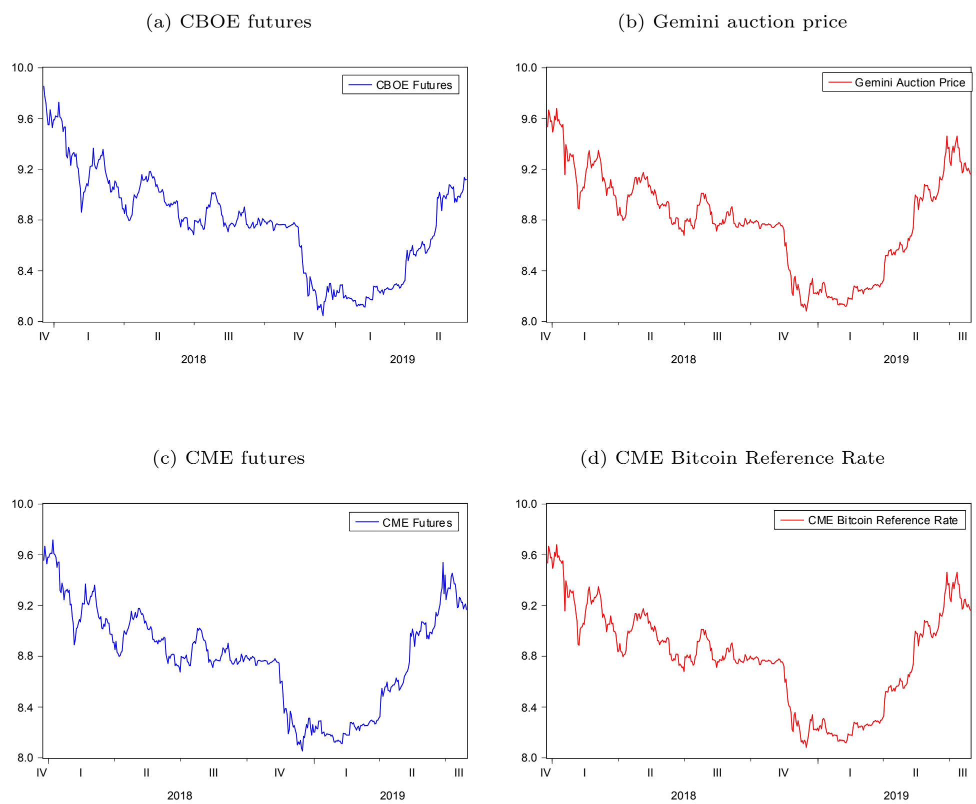

Figure 1: Time series plot of the CBOE futures prices, Gemini auction price, the CME futures prices and the CME Bitcoin Reference Rate prices in natural logarithmic scale.

Table 2: Descriptive statistics of the daily returns for spot and futures markets.

	Gemini auction price	CBOE futures	BRR	CME futures
Mean	-0.0018	-0.0019	-0.0009	-0.0009
Median	0.0000	0.0000	-0.0004	0.0000
Std.Dev.	0.0470	0.0479	0.0476	0.0514
Skewness	-0.1906	-0.1493	-0.0764	-0.3198
Kurtosis	6.4944	6.2973	7.1780	7.0927
JB	201.8147***	179.0373***	302.2371***	296.7135***
$LB^2(12)$	19.833***	20.562*	89.033***	51.658***

Daily returns are calculated as the first order differences of log daily prices. *Std.Dev.*, standard deviation. *JB*, the Jarque-Bera test statistic for normality. $LB^2(12)$ denote the Ljung-Box Q test statistic for return squares up to lag order 12. *** denotes significance at the 1% level.

2.2. Method

2.2.1. Time-varying Granger causality tests

The following section is taken from Shi et al. (2018). We can write an unrestricted VAR(p) in multi-variate regression format simply as:

$$\mathbf{y}_t = \Pi \mathbf{x}_t + \boldsymbol{\varepsilon}_t, \qquad t = 1, \ldots, T \tag{1}$$

where $\mathbf{y}_t$=$(\mathrm{y}_{1t}, \mathrm{y}_{2t})^{'}$, $\mathbf{x}_t = (1, \mathbf{y}_{t-1}^{'}, \mathbf{y}_{t-2}^{'}, \ldots, \mathbf{y}_{t-p}^{'})^{'}$, and $\mathbf{\Pi}_{2\times(2p+1)}$=$[\Phi_0, \Phi_1, \ldots, \Phi_p]$. Let $\hat{\mathbf{\Pi}}$ be the ordinary least squares estimator of $\mathbf{\Pi}$, $\hat{\boldsymbol{\Omega}} = \boldsymbol{T^{-1}} \sum_{\boldsymbol{t=1}}^{\boldsymbol{T}} \hat{\varepsilon}_t \hat{\varepsilon}_t^{'}$ with $\hat{\varepsilon}_t = \mathbf{y}_t - \hat{\mathbf{\Pi}} \mathbf{x}_t$ and $\mathbf{X}^{'} = [\mathbf{x}_1, \ldots, \mathbf{x}_T]$ be the observation matrix of the regressors in Equation 1. In order to test the null hypothesis that y_{2t} does not Granger cause y_{1t}, the Wald test for such restrictions can be denoted as:

$$\boldsymbol{W} = \left[\mathbf{R}\mathrm{vec}(\hat{\mathbf{\Pi}})\right]^{'} \left[\mathbf{R}\left(\hat{\Omega} \otimes \left(\mathbf{X}^{'}\mathbf{X}\right)^{\text{-1}}\right)\mathbf{R}^{'}\right]^{\text{-1}} \left[\boldsymbol{R}\mathrm{vec}(\hat{\Pi})\right], \tag{2}$$

where $\mathrm{vec}(\hat{\Pi})$ denotes the (row vectorized) $2(2p+1) \times 1$ coefficients of $\hat{\Pi}$ and $\boldsymbol{R}$ is the $p \times 2(2p+1)$ matrix. Each row picks one of the coefficients to set to zero under the non-causal null hypothesis. There are p coefficients on the lagged values of y_{2t} in Equation 1.

Following the recent bubble detection tests of Phillips et al. (2015), Shi et al. (2018) develop three tests based on the supremum norm (sup) of a series of recursively evolving Wald statistics for detecting changes in causal relationships using a forward recursive, a rolling window and a recursive evolving algorithm. If the Ward statistic sequence exceeds its corresponding critical value, a significant change in causality is detected. The origination (termination) date of a change in causality is identified as the first observation whose test statistic value exceeds (goes below) its corresponding critical values.

The Wald statistic obtained for each subsample regression over $[f_1, f_2]$ with a sample size fraction of f_W $(f_W = f_2 - f_1 \geq f_0)$ is denoted by $\mathcal{W}_{f_2}(f_1)$ and the sup Ward statistic is defined as:

$$\mathcal{SW}_f(f_0) = \sup_{(f_1, f_2) \in \Lambda_0, f_2 = f} \{\mathcal{W}_{f_2}(f_1)\}, \tag{3}$$

where $\Lambda_0 = \{(f_1, f_2) : 0 < f_0 + f_1 \leq f_2 \leq 1, \text{and} \quad 0 \leq f_1 \leq 1 - f_0\}$ for some minimal sample size $f_0 \in (0, 1)$ in the regressions. This is known as the recursive evolving procedure.

Let f_e and f_f denote the origination and termination points in the causal relationship, which are estimated as the first chronological observation whose test statistic respectively exceeds or falls below the critical value. The dating rules of the rolling and recursive evolving algorithms are given as:

$$\text{Rolling} : \hat{f}_e = \inf_{f \in [f_0, 1]} \{f : \mathcal{W}_f(0) > \text{cv}\} \qquad \text{and} \qquad \hat{f}_f = \inf_{f \in \left[\hat{f}_e, 1\right]} \{f : \mathcal{W}_f(0) < \text{cv}\}, \tag{4}$$

$$\text{Recursive Evolving} : \hat{f}_e = \inf_{f \in [f_0, 1]} \{f : \mathcal{SW}_f(0) > \text{scv}\} \qquad \text{and} \qquad \hat{f}_f = \inf_{f \in \left[\hat{f}_e, 1\right]} \{f : \mathcal{SW}_f(0) < \text{scv}\}, \tag{5}$$

where *cv* and *scv* are the corresponding critical values of the $\mathcal{W}_f$ and $\mathcal{SW}_f$ statistics. For multiple switches, the origination and termination dates are calculated in a similar fashion. As Shi et al. (2019) suggest, the power of the recursive evolving and rolling window approaches are much higher than that of the forward recursive testing procedure, and the recursive evolving algorithm offers the best finite sample performance. Hence, we investigate the potential causal relationship using these two procedures in this paper.

In estimating the bivariate VAR and implementing tests of Granger causality, the lag order is selected using the Bayesian information criterion (BIC) with the maximum lag length 12. The minimum window size f_0 is set to 0.2. The critical values are obtained from a bootstrapping procedure with 499 replications. The empirical size is 5% and is controlled over a three-month period.

2.2.2. Measurement of Price Discovery

Let Y_t be an $n \times 1$ vector of $I(1)$ series and assume that there exist $n-1$ cointegrating vectors; that is, Y_t contains a single common stochastic trend (Stock & Watson, 1988). Then Y_t can be specified in the following vector error correction model (VECM) (Engle & Granger, 1987):

$$\Delta Y_t = \pi Y_{t-1} + \sum_{i=1}^{k} A_i \Delta Y_{t-i} + \varepsilon_t, \tag{6}$$

where $\pi = \alpha\beta^T$. α and β are $n \times (n-1)$ matrices with $n-1$ non-zero eigenvalues. β contains $(n-1)$ cointegrating vectors such that $\beta^T Y_{t-1}$ consists of $(n-1)$ cointegrating equations. Each column of α is comprised of adjustment coefficients. The covariance matrix of the error term is given by $\Omega = E\left[\varepsilon_t \varepsilon_t^T\right]$, where $E\left[.\right]$ is the expectation operator. Following Stock & Watson (1988) and Hasbrouck (1995), Equation 6 can be transformed into the following vector moving average (VMA) model:

$$\Delta Y_t = \Psi(L)\varepsilon_t, \tag{7}$$

$$Y_t = Y_0 + \Psi(1)\sum_{i=1}^{t}\varepsilon_i + \Psi^*(L)\varepsilon_t, \tag{8}$$

According to the Engle-Granger representation theorem Engle & Granger (1987), $\Psi(1)$ has the following important properties due to the cointegrated unit-root series (De Jong, 2002; Lehmann, 2002):

$$\beta_T\Psi(1) = 0 \quad \text{and} \quad \Psi(1)\alpha = 0. \tag{9}$$

More importantly, $\Psi(1)\varepsilon_t$ in Equation 8 represents the long run impact of innovations on the unit-root series (Hasbrouck, 1995). This term is the major focus of different information share measures.

Hasbrouck Information (IS)

In Hasbrouck (1995), all the prices are equal in equilibrium because these series correspond to the prices of the same security being traded in multiple markets. This would impose special restrictions on cointegrating matrix β. That is, each of the pairwise cointegrating vector in β is (1, -1). Thus, Equation 9 implies that the rows of $\Psi(1)$ are identical. Let $\psi = (\psi_1, \psi_2, \ldots, \psi_n)$ be the identical row of $\Psi(1)$. Then $\Psi\varepsilon_t$ represents the long-run impact innovations on each of the price series. Assuming that the covariance matrix Ω is diagonal (i.e., the innovations are independent), the IS of market j is defined as:

$$S_j = \frac{\psi_j^2\Omega_{jj}}{\psi\Omega\psi^T}, \tag{10}$$

where ψ_j is the jth element of the row vector ψ. $\psi\Omega\psi^T$ represents the variance of $\psi\varepsilon_t$. It can be decomposed as:

$$\psi\Omega\psi^T = \sum_{j=1}^{n}\psi_j^2\Omega_{jj}. \tag{11}$$

Note that since $\psi\varepsilon_t$ represents the long-run impact of innovations on unit-root series, the IS of market j is the proportion of variance of the long-run impact of innovations that is attributable to innovations of market j (Baillie et al., 2002). In other words, the IS of market j is the contribution of market j to the total variance of the common efficient price or permanent impact (Lien & Shrestha, 2014). We can observe that $\psi\Omega\psi^T$ consists of n terms in Equation 11. The first (last) represents the contribution to the common factor innovation from the first (last) market (Baillie et al., 2002).

When the covariance matrix is not diagonal, that is, the innovations are not independent, the IS of market j is given by Hasbrouck (1995),

$$S_j = \frac{([\psi F]_j)^2}{\psi\Omega\psi^T}, \tag{12}$$

where F is the Cholesky factorization of Ω and is the lower triangular matrix such that $\Omega = FF^T$. $[\psi F]_j$ is the jth element of the row vector ψF. Due to the use of Cholesky factorization, Hasbrouck (1995) considers the upper (lower) bound of series j's information share when series j is the first (last) variable in the factorization. That is, the upper (lower) bound of series j's information share appears when series j is the first (last) series in Y_t. This is known as the ordering problem where the calculation of IS using Equation 12 depends on the particular ordering of the series. Thus the IS measure of any market is not unique.

In addition, Baillie et al. (2002) provide easy means to calculate the upper (lower) bound of a market's information share in an n-variate system. Let $F = (f_ij)_{i,j=1,...,n}$ and γ_i be the element of the row vector of $\alpha_\perp^T$. The upper and lower bounds of the IS measure of each market j with $1 \leq j \leq n$ are given as follows:

$$IS(UB)_j = \frac{\left[\sum_{i=1}^n \gamma_i f_{i1}\right]^2}{\left[\sum_{i=1}^n \gamma_i f_{i1}\right]^2 + \left[\sum_{i=2}^n \gamma_i f_{i2}\right]^2 + \cdots + \left[\gamma_n f_{nn}\right]^2}, \tag{13}$$

$$IS(LB)_j = \frac{\left[\gamma_n f_{nn}\right]^2}{\left[\sum_{i=1}^n \gamma_i f_{i1}\right]^2 + \left[\sum_{i=2}^n \gamma_i f_{i2}\right]^2 + \cdots + \left[\gamma_n f_{nn}\right]^2}. \tag{14}$$

As can be seen in Equations 13 and 14, the upper bound incorporates the market's own contribution represented by $f_1 1$ and its correlation with the other series as indicated by $f_i 1 (i = 2, \ldots, n)$. The lower bound only takes account of the series' "pure" contribution that does not correlate with the other series as represented by $f_n n$. We can also observe that the higher the correlation, the greater (smaller) the upper (lower) bound (Baillie et al., 2002).

Generalised Information Share (GIS)

Lien & Shrestha (2014) propose a new measure of information share to resolve the ordering problem of Hasbrouck information share. The new measurement is called generalised modified information share (GIS). GIS utilises a different factor structure that is based upon the correlation matrix of innovations instead of the covariance matrix. The IS measures illustrated thus far depend on the special restrictions imposed on the cointegrating matrix β. That is, each of the pairwise cointegrating vectors in β is (1,-1), which results in the rows of $\psi(1)$ to be identical. However, this assumption is restrictive since the one-to-one cointegrating relationship does not necessarily hold in the real world. Lien & Shrestha (2014) propose a new IS measure that does not require the cointegrating vector of each pair of series to be (1, -1). Therefore, such new measure can apply to series that do not have the one-to-one cointegrating relationships between them.

Suppose that the cointegrating matrix β contains a diagonal matrix $\Gamma_{(n-1)}$ and an $(n-1)$ column vector $\iota_{(n-1)}$. $\Gamma_{(n-1)} = \text{diag}(\theta_1, \theta_2, \ldots, \theta_{(n-1)})$ and $\iota_{(n-1)} = [1, \ldots, 1]^T$. Then β can be represented by:

$$\beta^T_{(n-1)\times n} = \left[\iota_{(n-1)} : -\Gamma_{(n-1)}\right]. \tag{15}$$

Note that Equation 15 implies that Y_t has $(n-1)$ cointegrating relationships; that is, Y_t has a single common stochastic trend. It is also worth noting that the cointegrating matrix given by Equations 15 has less restrictive condition than the one used to obtain the IS and MIS.

Combining with Equation 9, Equation 15 implies that the rows of $\Psi(1)$ are not identical. Let ψ^g_i be the ith row of $\Psi(1)$. Then the following relationship is obtained:

$$\psi^g_i = \theta_{i-1}\psi^g_i, \quad i = 2, \ldots, n. \tag{16}$$

Thus the long-run impact of innovations on the ith series is:

$$\psi^g_i \varepsilon_t = \psi^g_1 \theta^{-1}_{i-1} \varepsilon_t, \quad i = 1, \ldots, n, \tag{17}$$

where θ_0=1 and ψ^g_i is the first row of $\Omega(1)$.

When the innovations are independent, the variance of long-run impact on the ith series is:

$$\text{Var}(\psi^g_i \varepsilon_t) = \psi^g_i \Omega \psi^{g^T}_i = \sum_{j=1}^{n} \psi^2_{ij}\Omega_{jj} = \theta^{-2}_{i-1} \sum_{j=1}^{n} \psi^2_{1j}\Omega_{jj}, \tag{18}$$

where ψ_{ij} is the jth element of the row vector ψ^g_i and ψ_{1j} is the jth element of the row vector ψ^g_1. The contribution of the innovation of series j to the total variance of the common factor of series i is then represented by:

$$S^G_{j,i} = \frac{\psi^2_{1j}\Omega_{jj}}{\psi^g_1 \Omega \psi^{g^T}_1}, \tag{19}$$

$$S^G_{j,1} = S^G_{j,2} = \cdots = S^G_{j,n}, \quad j = 1, 2, \ldots, n. \tag{20}$$

$S_{j,i}^{G}$ is so called generalised information share (GIS) of series j which is independent of i. When the innovations are not independent, the GIS of series j can be calculated as:

$$S_j^G = \frac{\left(\psi_j^G\right)^2}{\psi_1^g \Omega \psi_1^{g^T}}, \tag{21}$$

where $\psi^G = \psi_1^g F^g$, $F^g = \hat{F} = \left[G\Lambda^{-1/2}G^T V^{-1}\right]^{-1}$, and ψ_j^G is the jth element of ψ^G. It should be noted that the GIS measure uses the factor structure same as the MIS; thus it would also be independent of the ordering problem.

We can compute the time-varying IS and GIS measures which are conditioned on the past information by replacing the time-invariant covariance matrix Ω of innovations used for calculating IS and GIS measures with its conditional counterpart obtained with Equation 29. We assume that error correction coefficients in Equation 6 are constant over the sample period in the calculation.

2.2.3. A time-varying cointegration test

Let S_t and F_t be the natural logarithms of daily prices of the spot and futures contacts, respectively. If the two series are integrated at the same order, a potential cointegration relationship where the cointegrating coefficient is time variant rather than static, is represented as:

$$S_t = \beta_0 + \beta\left(\frac{t}{n}\right)F_t + u_t, \tag{22}$$

where β_0 is a constant mean of the equation and u_t denotes the error correction term. $\beta\left(\frac{t}{n}\right)$ is the time-varying cointegrating coefficient associated with $\left(\frac{t}{n}\right)$ where t is the order of observation in the sample and n denotes the sample size. We have $\beta\left(\frac{t}{n}\right) = \beta(\lambda)$ such that $\lambda \in (0,1]$. Hence $\beta(\lambda)$ is a smooth function defined on [0,1]. According to Park & Hahn (1999), the time-series parameters, $\beta(\lambda)$, are approximated by the Fourier flexible form (FFF) functions,

$$\beta_k(\lambda) = \alpha_{k,1} + \alpha_{k,2}\lambda + \sum_{i=1}^{k}(\alpha_{k,2i+1}, \alpha_{k,2(i+1)})\varphi_i(\lambda), \tag{23}$$

where $\alpha_{k,j} \in R^2$ for $j = 1, 2, \ldots, 2(k+1)$, k is some positive integer. Let $\varphi_i(\lambda)$=$(\cos 2\pi i\lambda, \sin 2\pi i\lambda)$.

We also assume that:

$$\beta_k(\lambda) = f_k^{'}(\lambda)\alpha_k, \tag{24}$$

where $f_k(\lambda) = (1, \lambda, \varphi_1^{'}(\lambda), ; \varphi_k^{'}(\lambda))^{'}$ and $\alpha_k = (\alpha_{k,1}, \alpha_{k,2}, ; \alpha_{k,2(k+1)})^{'}$.

Therefore, Equation 22 can be written as:

$$S_t = \beta_0 + \alpha_k^{'} F_{kt} + u_{kt}, \tag{25}$$

where $F_{kt} = f_k(\lambda)F_t$, and $u_{kt} = u_t + [\beta(\lambda) - \beta_k(\lambda)]\, F_{kt}$.

Park & Hahn (1999) employ the superfluous regression approach to test the null hypothesis of the time-varying coefficient cointegration against the alternative of the spurious regression with non-stationary innovations. The corresponding test statistic is defined as:

$$\tau_1 = \frac{RSS_{TVC} - RSS^s_{TVC}}{\omega^2_*}, \tag{26}$$

where RSS_{TVC} and RSS^s_{TVC} are the sum of squared residuals from the CCR regression for Equation 25 and the same regression augmented with s additional superfluous regressors, respectively. Under the null hypothesis of a time-varying cointegration model, the limit distribution of τ_1 is a Chi-square distribution with s degree of freedom.

Alternatively, the null hypothesis of the validity of the time-invariant coefficient cointegration model, that is, $\beta\left(\frac{t}{n}\right)$ in Equation 22 is static over time, is tested by the test statistic as below:

$$\tau_2 = \frac{RSS_{FC} - RSS^s_{FC}}{\omega^2_*}, \tag{27}$$

where RSS_{FC} and RSS^s_{FC} are the sum of squared residuals from the CCR estimation of Equation 22 with the time-invariant cointegrating coefficient and the same regression augmented by s additional superfluous regressors, respectively. The limit distribution of τ_2 is the Chi-square distribution with s degree of freedom under the null. Moreover, the null hypothesis of the time-invariant cointegration model against the alternative of the time-varying model is tested with the null hypothesis $H_0 : \alpha_{k,2} = \alpha_{k,3}\ldots = \alpha_{k,2(k+1)} = 0$ in Equation 25 for a specific k.[7] The test statistic follows a Chi-square distribution with degree of freedom equal to the number of restrictions.

2.2.4. DCC-GARCH

To accommodate the time-varying second moments of return distribution, we use the Dynamic-Conditional-Correlation (DCC) BGARCH model proposed by Engle (2002) to model the conditional variance-covariance matrix of innovations of Equation 6. It should be noted that the conditional variance-covariance matrix underlie the calculation of time-varying information share measures. The

[7] In this paper, following the literature, we choose s to be 4. In addition, we choose k from a range between 1 and 5. The optimal k is picked based on the adjusted R-square of CCR.

DCC-BGARCH(1,1) model maybe written as:

$$\varepsilon_t \sim F(0, H_t) \tag{28}$$

$$H_t = D_t R_t D_t \tag{29}$$

$$D_t = \operatorname{diag}\left\{\sqrt{h_{11,t}}, \sqrt{h_{22,t}}\right\} \tag{30}$$

$$h_{ii,t} = \omega_{i0}^{'} + \omega_{i1}^{'}\varepsilon_{i,t-1}^{2} + \omega_{i2}^{'} h_{ii,t-1}, i = 1, 2, \tag{31}$$

$$R_t = \left(\operatorname{diag}\{Q_t\}\right)^{-1/2} Q_t \left(\operatorname{diag}\{Q_t\}^{-1/2}\right), \tag{32}$$

$$Q_t = (1 - \delta_1 - \delta_2)\bar{Q} + \delta_1 u_{t-1} u_{t-1}^{'} + \delta_2 Q_{t-1}, \tag{33}$$

$$Q_t = \begin{bmatrix} q_{11,t} & q_{12,t} \\ q_{21,t} & q_{22,t} \end{bmatrix}, \tag{34}$$

where $u_t = (u_{1t}, u_{2t})^{'}$ is a 2×1 vector of standardised residuals denoted by $u_{it} = \frac{\varepsilon_{it}}{\sqrt{h_{ii,t}}}(i = 1, 2)$. $h_{ii,t}$ is a standard individual GARCH process. Q_t is a 2×2 symmetric matrix where $q_{11,t}$ and $q_{22,t}$ denote the conditional variances of standardised disturbances u_{1t} and u_{1t} at time t, respectively. $q_{12,t}$ and $q_{21,t}$ is the conditional covariance between u_{1t} and u_{1t} at time t. $\overline{Q}$=$E\left[u_t u_t^{'}\right]$ is a 2×2 unconditional variance-covariance matrix of u_t. δ_1 and δ_2 are scalar parameters, and $\delta_1 \geq 0$, $\delta_2 \geq 0$, and $\delta_1 + \delta_2 \leq 1$ guarantee positive definiteness of the conditional variance–covariance matrix Q_t during the optimisation. δ_1 measures the presence of the conditional correlation and δ_2 examines the persistence of the time-varying nature.

Most of the applications of BGARCH models for estimating the optimal hedge ratio assume that error terms follow a bivariate conditional normal distribution. Bollerslev & Wooldridge (1992) show consistency and asymptotic normality of the quasi-maximum likelihood estimator (QMLE) of the GARCH model. However, QMLE will lose a lot of efficiency if the underlying conditional distribution is not normal (Engle & Gonzalez-Rivera, 1991; Park & Jei, 2010). Such efficiency loss might affect the forecasting of optimal hedge ratio based on the GARCH model estimated by QMLE. Typical distributional features the financial time-series data are excess kurtosis and asymmetry. In many applications of the GARCH model it is well known that conditional normality is not enough to explain excess kurtosis and asymmetry in financial data (Park & Jei, 2010).

In this paper, we employ a semi-nonparametric (SNP) approach to address the issue of excess kurtosis and non-zero skewness in the marginal return distribution. The DCC GARCH model is estimated via the maximization of log-likelihood of the multivariate SNP density function. In particular, a two-step estimation procedure is applied to obtaining estimates for the individual GARCH processes, conditional correlation matrix and marginal skewness and kurtosis parameters. First, the individual conditional variance equations are estimated via QMLE assuming Gaussian distribution and standardized innovations are obtained. Second, the parameters that capture the conditional correlation and other higher order moments are obtained via the log-likelihood maximization over the whole sample.

The log-likelihood of the multivariate SNP density that each observation at time t contributes to, without unnecessary constant components, is shown as:

$$\log(\mathrm{SNP}) = -\frac{1}{2}\log(R_t) - \frac{1}{2}u_t^{'} R_t^{-1} u_t + \log\left\{\sum_{i=1}^{2}\omega_i^{-1}\psi_i^2(x_{it})\right\}; \tag{35}$$

$$\psi_i(x_{it}) = 1 + s_i(x_{it}^3 - 3x_{it}) + k_i(x_{it}^4 - 6x_{it}^2 + 3); \tag{36}$$

$$\omega_i = 1 + s_i^2 + k_i^2; \tag{37}$$

$$x_t = (x_{1t}, x_{2t})^{'} = R_t^{-1/2} u_t, \tag{38}$$

where $i = 1, 2$. R_t is conditional correlation matrix defined by Equation 32. u_t is a vector of standardized innovations of the DCC-GARCH model. s_i and k_i $(i = 1, 2)$ are marginal skewness and kurtosis parameters, respectively.

3. Results

3.1. Time-varying Granger causality

We undertake ADF and PP unit root tests to check the stationarity of log futures and spot prices and conclude that all variables are $I(1)$.[8] As suggested in Shi et al. (2019), we conduct the analysis based on a VAR model that allows for possibly integrated data, and set the lag addition parameter d to unity.

We first concentrate on the CBOE market and test for any causal effects from the Gemini auction price (spot prices) to the CBOE futures prices. The time-varying Wald test statistics for causal effects from Bitcoin spot prices to CBOE futures prices along with their bootstrapped critical values are shown in Figure 2. These two rows illustrate the sequences of test statistics obtained from the rolling window and recursive evolving procedures respectively, while the columns of the figure refer to the two different assumptions for the residual error term (homoskedasticity and heteroskedasticity) for the VAR. Sequences of the test statistics start from April 2018. Under different model and error assumptions in Figure 2, the test statistics of the predictive power of spot prices on the CBOE futures prices are always below their bootstrapped critical values, suggesting there is no evidence to reject the null hypothesis of no Granger causality in all cases. As a result, date-stamping results from

[8]Unit root results are not shown here to save space. They are available upon request.

Figures 2a, to 2d suggest that spot prices cannot predict the CBOE futures prices, i.e., there is no causal relationship running from spot prices to the CBOE futures prices in all cases.

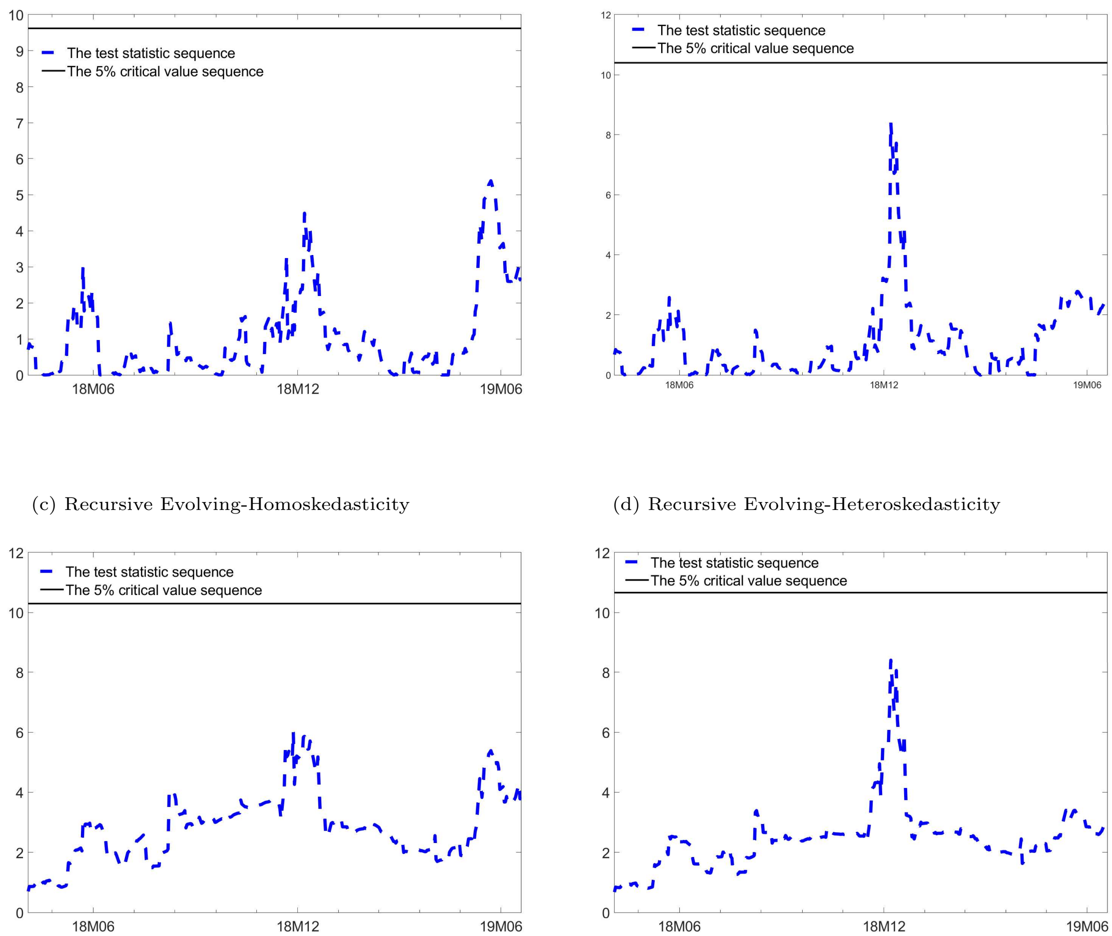

(a) Rolling Window-Homoskedasticity

(b) Rolling Window-Heteroskedasticity

(c) Recursive Evolving-Homoskedasticity

(d) Recursive Evolving-Heteroskedasticity

Figure 2: Tests for Granger causality running from the Gemini auction price (spot prices) to CBOE future prices (d=1).

We then consider the causal effects from the CBOE futures prices to spot prices as shown in Figure 3. First, there is little evidence of causality episodes based on the rolling window procedure as presented in Figures Figures 3a and 3b. Second, the recursive evolving approach offers some different results. As shown in Figure 3c, we find significant evidence of causality episodes running from the CBOE futures prices to spot prices from August 2018 to June 2019 as the test statistic exceeds the critical value sequences in August 2018 until the closure of the CBOE Bitcoin futures market in June 2019. As a result, the null hypothesis of no Granger causality can be rejected. Similarly, under the error assumption of heteroscedasticity, Figure 3d also presents significant evidence to support that the CBOE futures prices do Granger cause spot prices from November 2018 to June 2019. As noted in Shi et al. (2018), the recursive evolving window algorithm provides the most reliable results. Hence, we are confident in concluding that the CBOE futures prices Granger cause spot prices from August 2018/ November 2018 to the end of the CBOE futures market in June 2019.

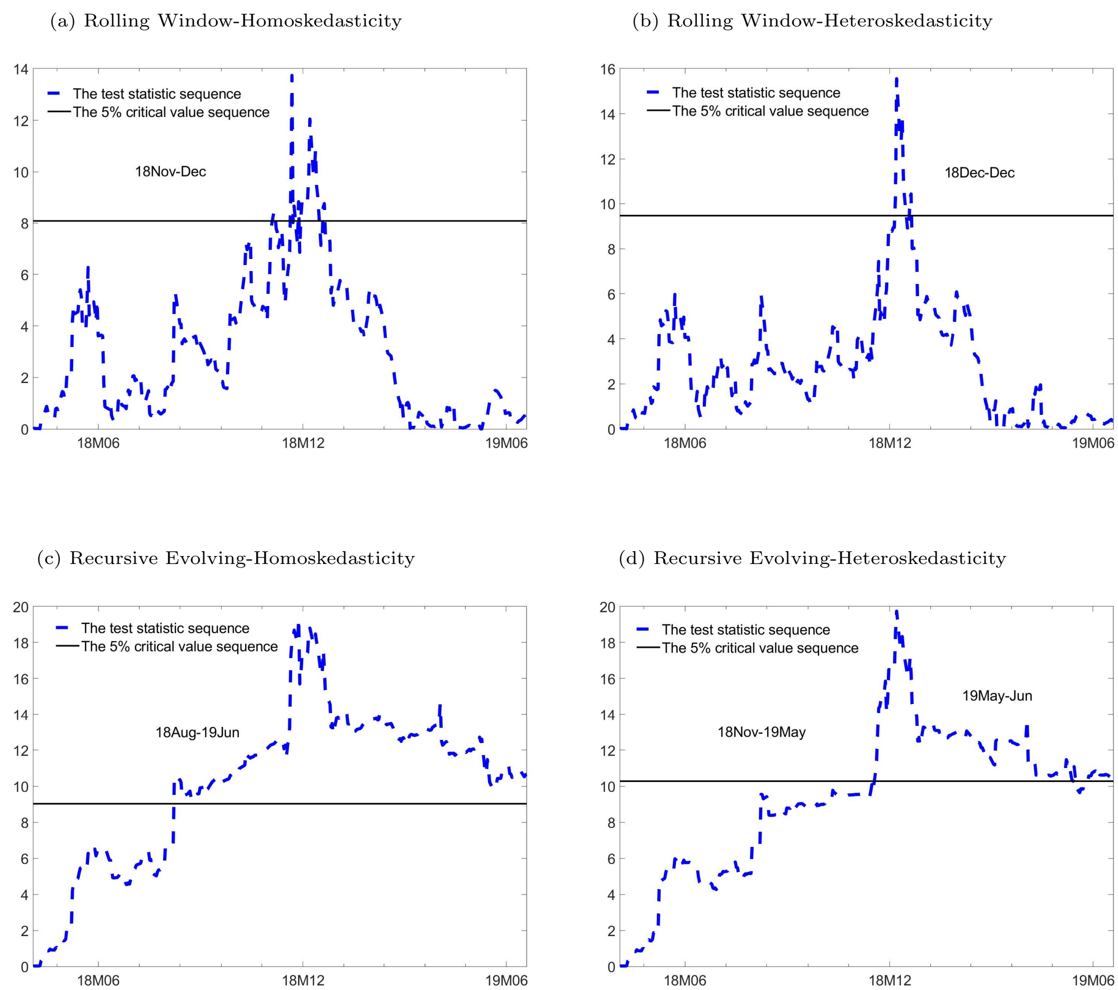

(a) Rolling Window-Homoskedasticity

(b) Rolling Window-Heteroskedasticity

(c) Recursive Evolving-Homoskedasticity

(d) Recursive Evolving-Heteroskedasticity

Figure 3: Tests for Granger causality running from the CBOE future to the Gemini auction price (spot prices) (d=1).

As stated above, the spot and futures prices of the CME are different from of those used for the CBOE. The conclusions drawn for the CBOE market do not necessarily hold for those of the CME market. Next, therefore, we carry out an analysis using the CME futures prices and CME BRR to explore the causal relationship between futures and spot markets with the results presented as in

Figure 4 and Figure 5. Figure 4 considers causality running from spot prices to the CME futures prices. As shown in Figure 4, we find quite similar results based on different testing procedures and error assumptions. For example, when we look at the date-stamping outcomes in Figure 4a and Figure 4b, the rolling window approach identifies an episode of causality between March 2019 and June 2019 under two error assumptions. When the recursive evolving procedure is applied as in Figure 4c and Figure 4d, we also identify an episode of causality from March 2019 to July 2019. Based on the above results, we can conclude that spot prices Granger cause the CME futures prices from March 2019 to June/July 2019.

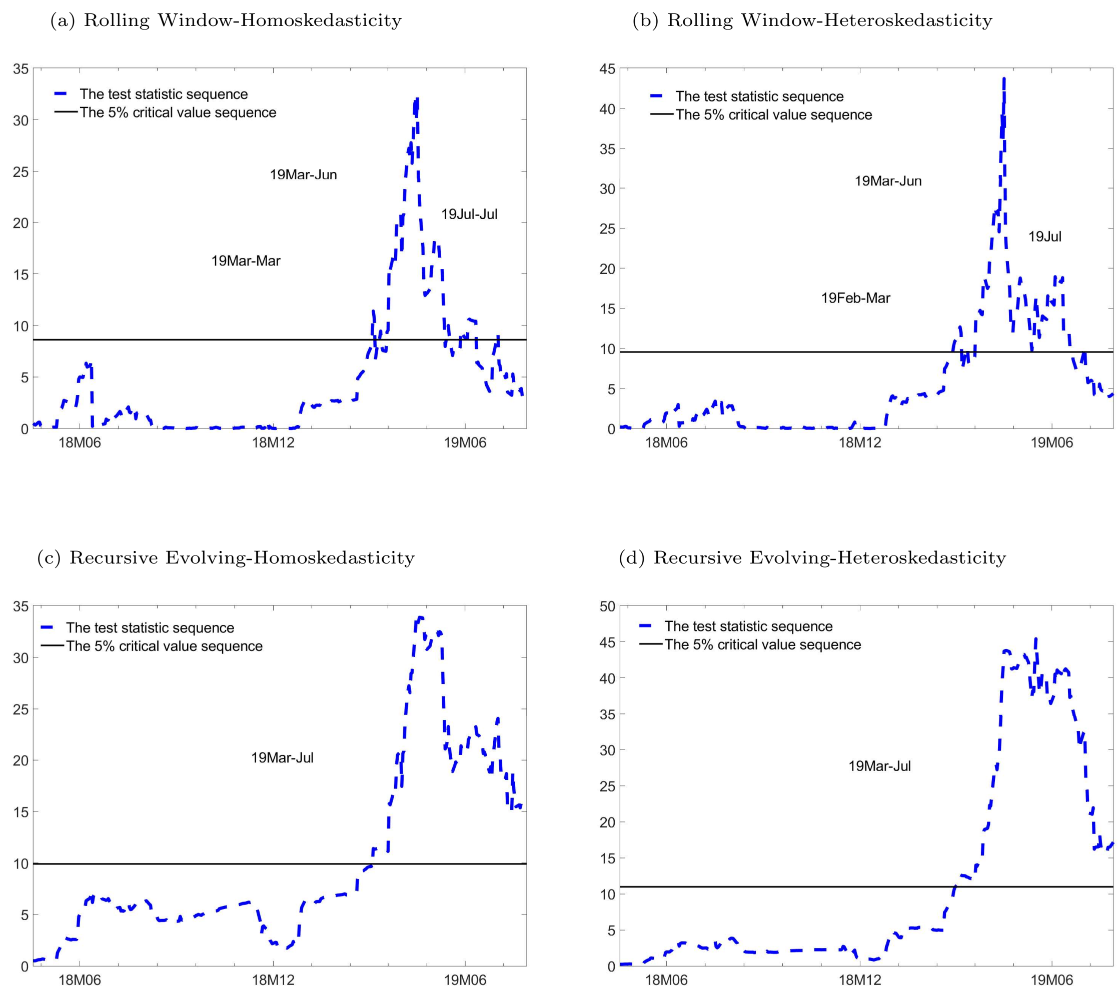

Figure 4: Tests for Granger causality running from the BRR (spot prices) to CME futures prices (d=1).

Finally, we conduct an analysis of Granger causality running from the CME futures to spot prices.

(a) Rolling Window-Homoskedasticity

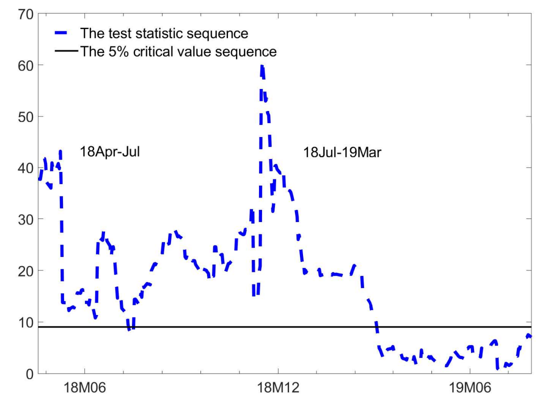

(b) Rolling Window-Heteroskedasticity

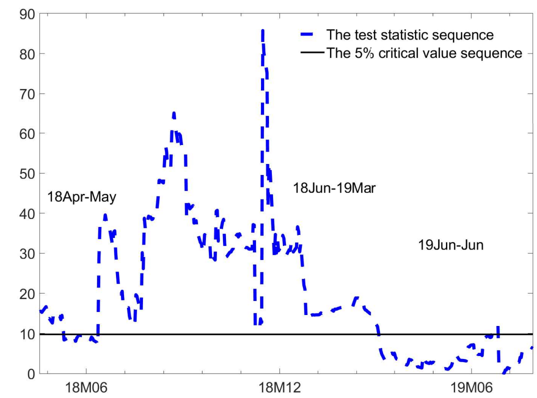

(c) Recursive Evolving-Homoskedasticity

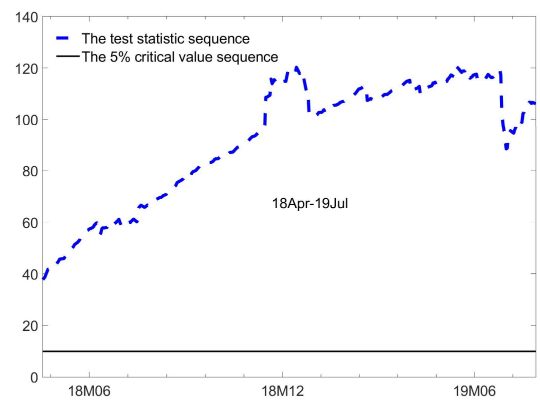

(d) Recursive Evolving-Heteroskedasticity

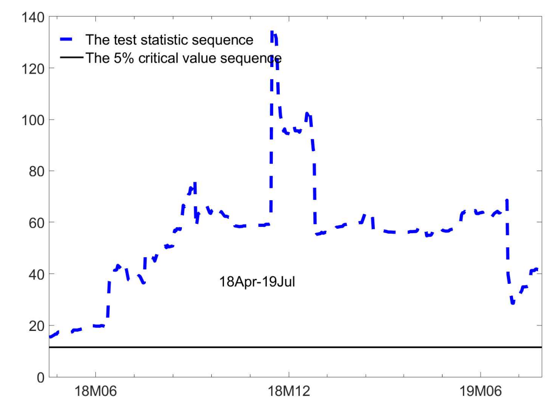

Figure 5: Tests for Granger causality running from the CME futures to the BRR (spot prices) (d=1).

Interestingly, we obtain significant evidence to reject the null of no causality from the CME futures to spot prices as presented in Figure 5. The rolling window approach finds an episode of causality between April 2018 and March 2019 in Figure 5a and Figure 5b with some small breaks. What is even more interesting is that the recursive evolving approach identifies an episode of causality for the whole period between April 2018 and July 2019 as shown in Figure 5c and Figure 5d. It is clear that our results are robust to different error assumptions. As the recursive evolving approach has higher power over the rolling window approach, we prefer the results obtained from the recursive evolving approach. Our results, therefore, suggest that the CME futures prices lead spot prices in the short term within the context of time-varying Granger causality.

The results from time-varying Granger causality tests present some very important findings. The key results for the CBOE and CME markets are summarzied as follows:

- CBOE market
  1. There are no causality episodes running from the Gemini auction price (spot prices) to the CBOE futures prices;
  2. The recursive evolving approach detects an episode (August/November 2018-June 2019) running from the CBOE futures prices to spot prices;
  3. Overall, the CBOE futures market dominates the spot market in terms of causality from August/November 2018 to June 2019.

- CME market
  1. There is a causality episode running from the BRR (spot prices) to the CME futures prices (March 2019-June/July 2019);
  2. The rolling window approach detects an episode (April 2018-March 2019) and recursive evolving approach detects an episode (April 2018-July 2019) running from the CME futures prices to spot prices;
  3. There is bi-directional causal relationship between spot price and the CME futures prices;
  4. Compared with duration of causal episodes and the magnitude of the test statistics in Figure 4 and Figure 5, the CME futures market dominates the underlying spot market in terms of causality.

3.2. Time-varying cointegration

(a) Time-varying cointegration coefficient β_{CBOE} (b) Time-varying cointegration coefficient β_{CME}

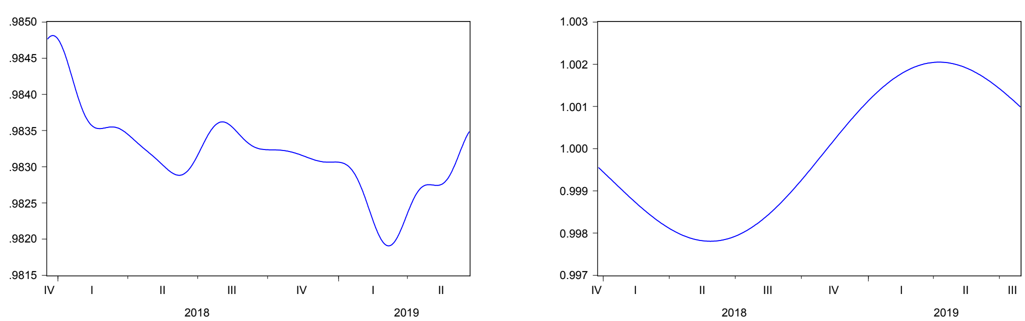

Figure 6: Time-varying cointegration coefficient β between spot and futures markets (CBOE and CME).

We employ Park & Hahn's (1999) procedure to test for the existence of cointegration permitting a time-varying cointegrating coefficient. We present the movements of the time-varying cointegration coefficients between the futures and spot markets in Figure 6. The time-varying cointegration coefficients of β_{CBOE} and β_{CME} for the two futures markets are shown as Figure 6a and Figure 6b, respectively. It seems that the patterns of β_{CBOE} and β_{CME} are both non-linear and time-varying during the entire sample period.

We next present cointegration test results based one CBOE market of Park & Hahn (1999) in Table 3. As shown in Panel A of Table 3, we cannot reject the null hypothesis of a time-varying cointegration model as the p-value of τ_1 statistic is 0.1091, indicating a cointegration relationship under time-varying coefficients between the spot and CBOE futures markets. However the null hypothesis of the validity of the time-invariant coefficient cointegration model can be rejected as the p-value of τ_2 statistic is 0. Results from τ_2 provide the further support for a time-varying cointegration model. Alternatively, the null hypothesis of the time-invariant cointegration model against the alternative of the time-varying model is also tested with the null hypothesis $H_0 : \alpha_{k,2} = \alpha_{k,3} \ldots = \alpha_{k,2(k+1)} = 0$ when k=8.[9] The result from Panel A provides significant evidence to support a time-varying model as the p-value of a Chi-square statistic $\chi^2(2k+1)$ is 0. We, therefore, prefer the time-varying cointegration model rather than the time-invariant cointegration model.

We also obtain the similar result from Panel B of Table 3 for the CME markets. The null hypothesis of a time-varying cointegration model is not rejected as the p-value of τ_1 statistic is 0.3515, suggesting a cointegration relationship under time-varying coefficients between the spot and CME futures markets. On the other hand, the p-value of τ_2 statistic is 0, rejecting the null hypothesis of the time-invariant coefficient cointegration model. The results from τ_2 are in line with τ_1. The time-varying model is preferred over the time-invariant cointegration model for the CME futures markets as the Chi-square statistic $\chi^2(2k + 1)$ is significant at the 1% level.[10] Overall, we prefer to apply a time-varying cointegration model between Bitcoin spot and futures markets due to significant evidence as suggested by Table 3.

3.3. Time-varying Price Discovery

Results for the static (time-invariant) price discovery measures are summarised in Table 4. With respect to price discovery of the CBOE futures and spot markets in Panel A, the IS (upper bound,

[9] k is chosen to be 8 for the Park and Hahn test since it generates the highest adjusted R-square of the CCR under the null hypothesis. We also test the null when k is 1, 2, 3, . . . , 8 and find the results are qualitatively similar. We also try alternative choices for the equality test.

[10] In the test for the CME futures, the optimal value of k is chosen to be 1.

Table 3: Cointegration test under time-invariant and time-varying coefficients.

Panel A: CBOE futures	p-value
Time-varying coefficient	
τ_1	P_{τ_1}: 0.1091
Time-invariant coefficient	
τ_2	P_{τ_2}: 0.0000***
$H_0 : \alpha_{k,2} = \alpha_{k,3} = \cdots = \alpha_{k,2(k+1)}$	
$\chi^2(2k+1)$	$P_{\chi^2(2k+1)}$: 0.0000***
Panel B: CME futures	**p-value**
Time-varying coefficient	
τ_1	P_{τ_1}: 0.3515
Time-invariant coefficient	
τ_2	P_{τ_2}: 0.0000***
$H_0 : \alpha_{k,2} = \alpha_{k,3} = \cdots = \alpha_{k,2(k+1)}$	
$\chi^2(2k+1)$	$P_{\chi^2(2k+1)}$: 0.0000***

This table presents results of Park & Hahn (1999) test. τ_1 and τ_2 are calculated by Equation 26 and Equation 27, respectively. k in Panel A refers to the number of pairs of trigonometric polynomial functions in Equation 23. *** denotes significance at the 1% level.

Table 4: The static (time-invariant) estimates of price discovery measure for Bitcoin spot and two futures markets.

Panel A		**IS Measure**		**GIS Measure**
	Upper Bound	Lower Bound	Mid-point	
CBOE futures	0.9980	0.0077	0.5029	0.5216
Spot	0.9924	0.0020	0.4972	0.4784
Panel B		**IS Measure**		**GIS Measure**
	Upper Bound	Lower Bound	Mid-point	
CME futures	0.9540	0.0926	0.5233	0.5464
Spot	0.9074	0.0460	0.4767	0.4536

(a) Time-varying IS measure of the spot markets

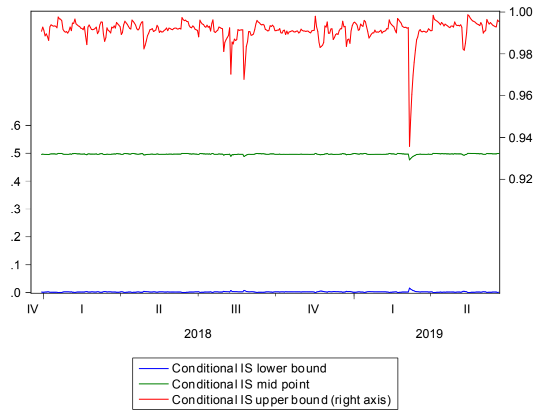

(b) Time-varying IS measure of the CBOE futures markets.

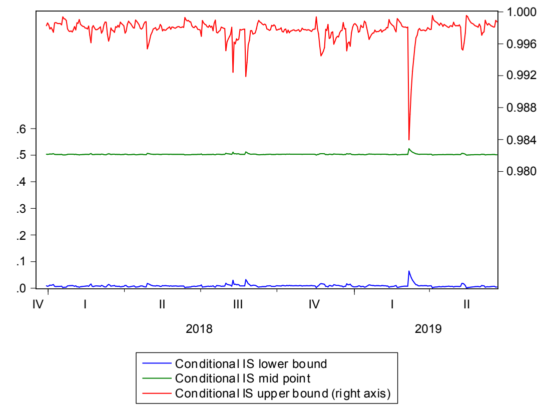

(c) Time-varying IS measures of mid point.

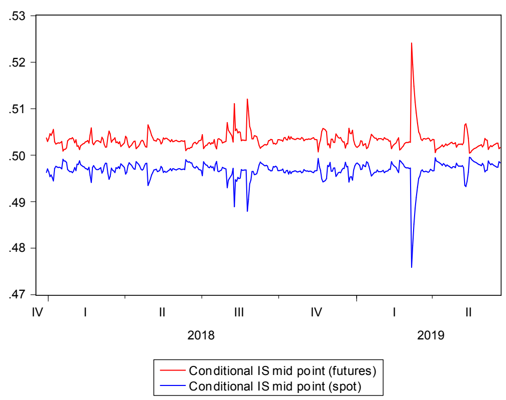

(d) Time-varying GIS measures of the spot and CBOE futures markets.

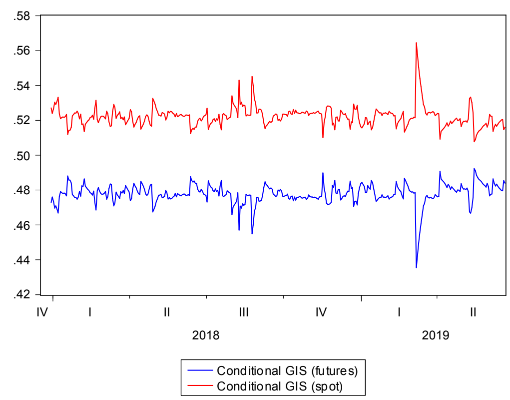

Figure 7: Time-varying IS and GIS measures of Bitcoin spot and CBOE futures markets.

lower bound and mid-point) and GIS measures of the CBOE futures are higher than those of spot markets. Hence, price discovery takes place in CBOE futures market rather than Bitcoin spot market. It should be pointed out that the CBOE futures market dominates the price discovery process. We then look at the results for the CME futures market in Panel B. It is clear that the IS (upper bound, lower bound and mid-point) and GIS measures of the CME futures are higher than those of spot markets, indicating that the CME futures market outperforms in terms of static information shares price discovery. In general, Table 4 suggests that both CBOE and CME futures markets lead the Bitcoin spot market. This finding is consistent with the results of time-varying Granger causality approaches reported in Section 3.1.

Table 5: The time-varying estimates of price discovery measure for spot and two futures markets.

Panel A		Mean	Sd	Max	Min
IS Measure					
	CBOE futures				
	Upper Bound	0.9977	0.0014	0.9995	0.9840
	Lower Bound	0.0087	0.0054	0.0643	0.0014
	Mid-point	0.5032	0.0020	0.5241	0.5004
	Spot				
	Upper Bound	0.9913	0.0054	0.9986	0.9357
	Lower Bound	0.0023	0.0014	0.0160	0.0005
	Mid-point	0.4968	0.0020	0.4996	0.4759
t-test of equality between mid point of the two markets	t-test	p-value			
	43.9975	0.0000			
	CME futures				
	Upper Bound	0.9544	0.0056	0.9709	0.9277
	Lower Bound	0.0934	0.0118	0.1888	0.0696
	Mid-point	0.5239	0.0064	0.5738	0.5110
	Spot				
	Upper Bound	0.9066	0.0118	0.9304	0.8112
	Lower Bound	0.0456	0.0056	0.0723	0.0291
	Mid-point	0.4761	0.0064	0.4890	0.4262
t-test of equality between mid point of the two markets	t-test	p-value			
	105.6303	0.0000			
Panel B		Mean	Sd	Max	Min
GIS Measure					
	CBOE futures	0.5222	0.0058	0.5645	0.5077
	Spot	0.4778	0.0058	0.4923	0.4355
t-test of equality between mid point of the two markets	t-test	p-value			
	105.9086	0.0000			
	CME futures	0.5475	0.0110	0.6214	0.5207
	Spot	0.4525	0.0110	0.4793	0.3786
t-test of equality between mid point of the two markets	t-test	p-value			
	122.0624	0.0000			

(a) Time-varying IS measure of the spot market

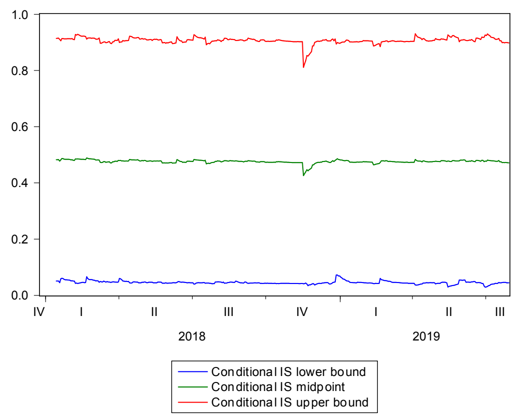

(b) Time-varying IS measure of the CME futures market.

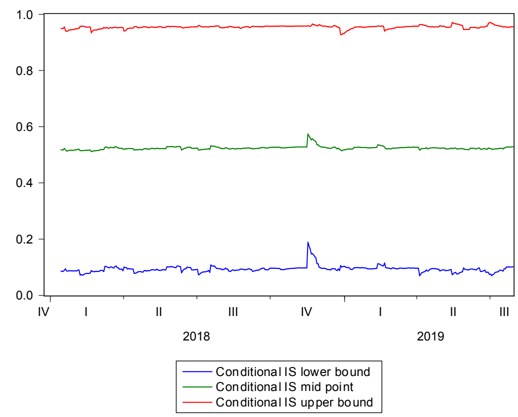

(c) Time-varying IS measures of mid point.

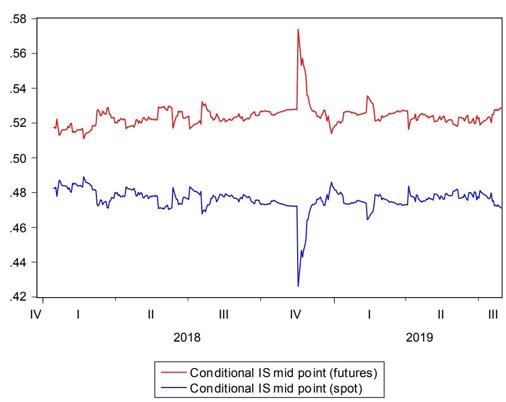

(d) Time-varying GIS measures of the spot and CME futures markets.

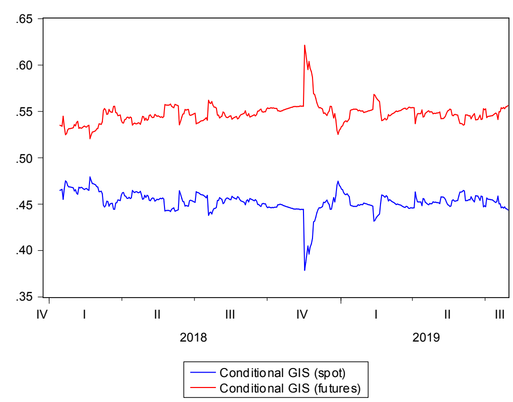

Figure 8: Time-varying IS and GIS measures of Bitcoin spot and CME futures markets.

Results of the time-varying price discovery measures are summarised in Table 5. As can be seen from Panel A, the mean, maximum and minimum estimates of upper bound, lower bound and mid-point of the IS measures for the CME futures are higher than those of spot markets. Similarly, the CBOE futures market outperforms the spot market in terms of conditional information shares as the mean, maximum and minimum estimates of upper bound, lower bound and mid-point of the IS measures for the CBOE futures market are also higher than those of the spot market. Hence, conditional IS measures suggest that price discovery mainly takes place in the Bitcoin futures markets, rather than spot counterpart. The results are consistent with static measures. In addition, standard deviations of the IS measures for the spot and futures markets are small, indicating that those measures are stable over the entire sample period. Results for the conditional GIS of Bitcoin spot and futures are shown in the Panel B of Table 5. The GIS results are similar to the IS measures of Panel A. Moreover, the GIS measures are stable given their small standard deviations. In addition, we test the equality of means of the conditional mid-point IS and that of conditional GIS between Bitcoin spot and futures markets. The t statistics are all significant for the IS and GIS measures, for both the CBOE and CME cases. The results indicate that the differences in dynamic price discovery performance between Bitcoin futures and spot markets are substantial, which confirms a leading role the futures markets play in the long-run information channels. Overall, both the CBOE and CME futures markets have higher means of the GIS than the spot counterpart, indicating that the Bitcoin futures markets dominate in the dynamic price discovery process.

Furthermore, the time-varying IS and GIS measures of the Bitcoin spot and two futures markets are depicted in Figure 7 and Figure 8, respectively. As shown in both figures, the values of the conditional series of the IS and GIS measures for futures markets are higher than those of the spot markets across time, which is consistent with the results of Table 6. We can, therefore, conclude that the Bitcoin futures markets dominate the dynamic price discovery process based upon time-varying information share measures. Overall, price discovery seems to occur in the Bitcoin futures markets rather than the underlying spot market based upona time-varying perspective, which is consistent with results obtained from the static (time-invariant) information share measures in Table 4.

The estimation result of the DCC-GARCH model with SNP approach is shown in Table 6. The model estimates are used to predict the conditional variances and covariances of Bitcoin spot and futures markets which determines conditional IS amd GIS measures. As can be seen from Panel A of the table, volatility clustering exists in all the markets, where the individual variances are driven by the arrival of new shocks. In addition, persistency of variances is significant for all four markets.

Panel B of Table 6 suggests that correlation between the Bitcoin spot and futures markets is conditioned on the past shocks as well as their own lagged values, given the significant estimates of δ_1 and δ_2. Moreover, the SNP approach significantly captures the excess kurtosis of return distribution. Skewness parameters are estimated, but none of them are significant. It suggests asymmetry of the distribution might not be a significant obstacle for model estimation. Finally, Panel D of Table 6 shows that there is no heteroscedasticity remaining in the standardised innovations, suggesting the entire model is now well specified.

Table 6: The DCC-GARCH-SNP model.

	CBOE		CME	
Coefs.				
Panel A: Conditional variances	i=1	i=2	i=1	i=2
$\omega_{io}^{'}$	7.74×10^{-5}	4.69×10^{-5}	$7.74{\times}10^{-5}$***	0.0001***
	(0.1222)	(0.1011)	(0.0000)	(0.0002)
$\omega_{i1}^{'}$	0.0291**	0.0158*	0.0561***	0.0536***
	(0.0453)	(0.0637)	(0.0000)	(0.0000)
$\omega_{i2}^{'}$	0.9321***	0.9577***	0.8883***	0.8765***
	(0.0000)	(0.0000)	(0.0000)	(0.0000)
Panel B: Conditional correlation				
δ_1	0.1474***		0.0170**	
	(0.0000)		(0.0426)	
δ_2	0.6779***		0.8380***	
	(0.0000)		(0.0000)	
Panel C: SNP distribution				
s_1	-0.4167		0.1794	
	(0.3509)		(0.5803)	
s_2	-0.106947		-0.1459	
	(0.7902)		(0.6388)	
k_1	4.9499		5.6004*	
	(0.1318)		(0.0807)	
k_2	5.8634		4.6873*	
	(0.1729)		(0.0567)	
Panel D: Residual diagnosis				
$LB^2(12)$	2.5025	2.0816	3.4686	4.9499
$ARCH(12)$	2.4730	2.0478	3.5544	4.9175

Notes: This table reports the estimation results of the bivariate DCC-GARCH-SNP model based upon Equation 29 to Equation 34. $Coefs.$ denotes coefficients. i=1 refers to the conditional variance equation of Bitcoin spot markets (Gemini auction price or BRR) while i=2 refers to the conditional variance equation of Bitcoin futures markets (CBOE or CME). $LB^2(12)$ is the Ljung-Box Q statistics of squared standardised residuals up to lag order 12. $ARCH(12)$ denotes the test statistic for testing the ARCH effect up to lag order 12. Figures in the parentheses are p-values. ***, **, and * denote significance at the 1%, 5% and 10% levels, respectively.

4. Conclusion

This paper investigates the existence of causal relationships, cointegration and price discovery between Bitcoin spot and futures of the CBOE and CME from December 2017 to June/July 2019 from a time-varying perspective for the first time in the literature.

Of particular importance from the results of this paper is that we offer more robust evidence to support our key findings. This paper presents three important findings as follows. First, the results from a recently proposed time-varying Granger causality test of Shi et al. (2018, 2019) suggest that the CBOE and CME futures prices Grange cause the underlying spot markets. For the CBOE market, the CBOE futures prices Granger cause spot prices between August/November 2018 and June 2019 based on the recursive evolving testing procedure. However, there are no causality episodes running from spot prices to the CBOE futures prices. For the CME market, there is a causality episode running from spot prices to the CME futures prices (March 2019-June/July 2019) using both rolling window and recursive evolving testing procedures. The rolling window approach detects an episode (April 2018-March 2019) and recursive evolving approach detects an episode (April 2018-July 2019) running from the CME futures prices to spot prices. There is a bi-directional causal relationship between spot price and the CME futures prices appears to exist. Compared with the duration of the causal episodes and the magnitude of the test statistics, the CME futures market appears to dominate the underlying spot market in terms of causality. Second, using the test of Park & Hahn (1999), we cannot reject the null hypothesis of a time-varying cointegration model allowing for time-varying cointegrating coefficients between the spot and two futures markets. Our results suggest that the time-varying cointegration model is preferred over the time-invariant (fixed) cointegration model. In other words, the time-varying cointegration model is better suited to describe the relationship between spot and futures markets. Third, we also find that Bitcoin futures markets dominate the price discovery process using a time-varying version based on information share measures of the IS and GIS types. Both the two information share measures indicate that price discovery takes place in the Bitcoin futures markets, rather than the spot market. Overall, these results indicate that the Bitcoin futures markets provide their functionality as expected, in terms of informational efficiency. The futures contracts can be an efficient tool for risk management of the underlying spot asset. Hence, our results deliver important implications for market participants and regulators.

References

Alexander, C., & Dakos, M. (2019). A critical investigation of cryptocurrency data and analysis. *Available at SSRN 3382828*, .

Ates, A., & Wang, G. H. (2005). Information transmission in electronic versus open-outcry trading systems: An analysis of US equity index futures markets. *Journal of Futures Markets*, *25*, 679–715.

Avino, D., Lazar, E., & Varotto, S. (2015). Time varying price discovery. *Economics Letters*, *126*, 18–21.

Baillie, R. T., Booth, G. G., Tse, Y., & Zabotina, T. (2002). Price discovery and common factor models. *Journal of Financial Markets*, *5*, 309–321.

Baur, D. G., & Dimpfl, T. (2019). Price discovery in bitcoin spot or futures? *Journal of Futures Markets*, .

Bell, A. R., Brooks, C., & Taylor, N. (2016). Time-varying price discovery in the eighteenth century: Empirical evidence from the London and Amsterdam stock markets. *Cliometrica*, *10*, 5–30.

Bohl, M. T., Salm, C. A., & Schuppli, M. (2011). Price discovery and investor structure in stock index futures. *Journal of Futures Markets*, *31*, 282–306.

Bollerslev, T., & Wooldridge, J. M. (1992). Quasi-maximum likelihood estimation and inference in dynamic models with time-varying covariances. *Econometric reviews*, *11*, 143–172.

Booth, G. G., So, R. W., & Tse, Y. (1999). Price discovery in the german equity index derivatives markets. *Journal of Futures Markets*, *19*, 619–643.

Cabrera, J., Wang, T., & Yang, J. (2009). Do futures lead price discovery in electronic foreign exchange markets? *Journal of Futures Markets*, *29*, 137–156.

Chan, K. (1992). A further analysis of the lead–lag relationship between the cash market and stock index futures market. *The Review of Financial Studies*, *5*, 123–152.

Chen, Y.-L., & Gau, Y.-F. (2009). Tick sizes and relative rates of price discovery in stock, futures, and options markets: Evidence from the Taiwan stock exchange. *Journal of Futures Markets*, *29*, 74–93.

Chen, Y.-L., & Gau, Y.-F. (2010). News announcements and price discovery in foreign exchange spot and futures markets. *Journal of Banking & Finance*, *34*, 1628–1636.

Corbet, S., Lucey, B., Peat, M., & Vigne, S. (2018). Bitcoin Futures—what use are they? *Economics Letters*, *172*, 23–27.

Covrig, V., Ding, D. K., & Low, B. S. (2004). The contribution of a satellite market to price discovery: Evidence from the Singapore exchange. *Journal of Futures Markets: Futures, Options, and Other Derivative Products*, *24*, 981–1004.

De Jong, F. (2002). Measures of contributions to price discovery: A comparison. *Journal of Financial markets*, *5*, 323–327.

Engle, R. (2002). Dynamic conditional correlation: A simple class of multivariate generalized autoregressive conditional heteroskedasticity models. *Journal of Business & Economic Statistics*, *20*, 339–350.

Engle, R. F., & Gonzalez-Rivera, G. (1991). Semiparametric ARCH models. *Journal of Business & Economic Statistics*, *9*, 345–359.

Engle, R. F., & Granger, C. W. (1987). Co-integration and error correction: representation, estimation, and testing. *Econometrica*, *55*, 251–276.

Garbade, K. D., & Silber, W. L. (1983). Price movements and price discovery in futures and cash markets. *The Review of Economics and Statistics*, *65*, 289–297.

Ghosh, A. (1993). Cointegration and error correction models: Intertemporal causality between index and futures prices. *Journal of futures markets*, *13*, 193–198.

Gonzalo, J., & Granger, C. (1995). Estimation of common long-memory components in cointegrated systems. *Journal of Business & Economic Statistics*, *13*, 27–35.

Hasbrouck, J. (1995). One security, many markets: Determining the contributions to price discovery. *The Journal of Finance*, *50*, 1175–1199.

Hauptfleisch, M., Putniņš, T. J., & Lucey, B. (2016). Who sets the price of gold? London or New York. *Journal of Futures Markets*, *36*, 564–586.

Kapar, B., & Olmo, J. (2019). An analysis of price discovery between Bitcoin futures and spot markets. *Economics Letters*, *174*, 62–64.

Kavussanos, M. G., Visvikis, I. D., & Alexakis, P. D. (2008). The lead-lag relationship between cash and stock index futures in a new market. *European Financial Management*, *14*, 1007–1025.

Koutmos, G., & Tucker, M. (1996). Temporal relationships and dynamic interactions between spot and futures stock markets. *Journal of Futures Markets*, *16*, 55–69.

Lehmann, B. N. (2002). Some desiderata for the measurement of price discovery across markets. *Journal of Financial Markets*, *5*, 259–276.

Lien, D., & Shrestha, K. (2014). Price discovery in interrelated markets. *Journal of Futures Markets*, *34*, 203–219.

Park, J. Y., & Hahn, S. B. (1999). Cointegrating regressions with time varying coefficients. *Econometric Theory*, *15*, 664–703.

Park, S. Y., & Jei, S. Y. (2010). Estimation and hedging effectiveness of time-varying hedge ratio: Flexible bivariate garch approaches. *Journal of Futures Markets*, *30*, 71–99.

Phillips, P. C. B., Shi, S., & Yu, J. (2015). Testing for multiple bubbles: Historical episodes of exuberance and collapse in the S&P 500. *International Economic Review*, *56*, 1043–1078.

Pizzi, M. A., Economopoulos, A. J., & O'Neill, H. M. (1998). An examination of the relationship between stock index cash and futures markets: A cointegration approach. *Journal of Futures Markets*, *18*, 297–305.

Putniņš, T. J. (2013). What do price discovery metrics really measure? *Journal of Empirical Finance*, *23*, 68–83.

Rosenberg, J. V., & Traub, L. G. (2009). Price discovery in the foreign currency futures and spot market. *The Journal of Derivatives*, *17*, 7–25.

Shi, S., Hurn, S., & Phillips, P. C. (2019). Causal change detection in possibly integrated systems: revisiting the money-income relationship. *Journal of Financial Econometrics*, .

Shi, S., Phillips, P. C., & Hurn, S. (2018). Change detection and the causal impact of the yield curve. *Journal of Time Series Analysis*, *39*, 966–987.

Silber, W. L. (1981). Innovation, competition, and new contract design in futures markets. *Journal of Futures Markets*, *1*, 123–155.

Stock, J. H., & Watson, M. W. (1988). Testing for common trends. *Journal of the American statistical Association*, *83*, 1097–1107.

Stoll, H. R., & Whaley, R. E. (1990). The dynamics of stock index and stock index futures returns. *Journal of Financial and Quantitative Analysis*, *25*, 441–468.

Taylor, N. (2011). Time-varying price discovery in fragmented markets. *Applied Financial Economics*, *21*, 717–734.

Tse, Y. (1999). Price discovery and volatility spillovers in the djia index and futures markets. *Journal of Business Finance & Accounting*, *19*, 911–930.

Tse, Y., Bandyopadhyay, P., & Shen, Y.-P. (2006). Intraday price discovery in the DJIA index markets. *Journal of Business Finance & Accounting*, *33*, 1572–1585.

Wahab, M., & Lashgari, M. (1993). Price dynamics and error correction in stock index and stock index futures markets: A cointegration approach. *Journal of Futures Markets*, *13*, 711–742.

Xu, F., & Wan, D. (2015). The impacts of institutional and individual investors on the price discovery in stock index futures market: Evidence from China. *Finance Research Letters*, *15*, 221–231.

Yan, B., & Zivot, E. (2010). A structural analysis of price discovery measures. *Journal of Financial Markets*, *13*, 1–19.

Yang, J., Bessler, D. A., & Leatham, D. J. (2001). Asset storability and price discovery in commodity futures markets: a new look. *Journal of Futures Markets*, *21*, 279–300.